

Fermi National Accelerator Laboratory

FERMILAB-Conf-93/308

Theory, Technology and Technique of Stochastic Cooling

John Marriner

*Fermi National Accelerator Laboratory
P.O. Box 500, Batavia, Illinois 60510*

October 1993

Submitted to the *Workshop on Beam Cooling and Related Topics*, Montreux, Switzerland, October 3-8, 1993

Disclaimer

This report was prepared as an account of work sponsored by an agency of the United States Government. Neither the United States Government nor any agency thereof, nor any of their employees, makes any warranty, express or implied, or assumes any legal liability or responsibility for the accuracy, completeness, or usefulness of any information, apparatus, product, or process disclosed, or represents that its use would not infringe privately owned rights. Reference herein to any specific commercial product, process, or service by trade name, trademark, manufacturer, or otherwise, does not necessarily constitute or imply its endorsement, recommendation, or favoring by the United States Government or any agency thereof. The views and opinions of authors expressed herein do not necessarily state or reflect those of the United States Government or any agency thereof.

THEORY, TECHNOLOGY, AND TECHNIQUE OF STOCHASTIC COOLING

John Marriner

Fermilab* , P.O. Box 500, Batavia, IL 60510

ABSTRACT

The theory and technological implementation of stochastic cooling is described. Theoretical and technological limitations are discussed. Data from existing stochastic cooling systems are shown to illustrate some useful techniques.

1. THEORY

1.1 Introduction

The theory of stochastic cooling has been discussed by a number of authors [1,2,3,4,5,6,7]. I will try to describe the theory and to make the results seem plausible, but I will not give a detailed derivation of the results.

A prototypical transverse stochastic cooling system is shown in Fig. 1. The system senses the particle position at the pickup by measuring the difference in induced current between the two pickup electrodes. The electronic signal is amplified and applied to the kicker electrode when the particle passes between the electrodes. Transverse electric and magnetic fields in the kicker deflect the particle. The angular deflection at the kicker will decrease the amplitude of the betatron oscillations provided that it has the correct sign.

1.2 Schottky Signals

An understanding of Schottky signals is central to the understanding of stochastic cooling. A particle passing a point in the ring with revolution frequency makes a current

$$\begin{aligned} i(t) &= e \sum_{n=-\infty}^{\infty} \delta\left(t + \tau - \frac{n}{f_0}\right) \\ &= ef_0 \left[1 + 2 \sum_{n=1}^{\infty} \cos n\omega_0(t + \tau) \right]. \end{aligned} \quad (1)$$

The current consists of an infinite series of lines at multiples of the revolution frequency. If we consider a beam of particles with random values of τ then the ac current will be nearly zero because of the random phase factor in Eq. (1). The rms current is not zero and is known as the Schottky current. In a beam the revolution frequencies are similar but not identical for all particles. Thus, the Schottky currents organize themselves into bands around the average revolution frequency. The rms current per Schottky band for a beam of N particles is

$$P_l = 2Ne^2 f_0^2. \quad (2)$$

The betatron motion of a particle in the beam at the observation point is given by

$$x(t) = A \cos(\omega_0 Q t + \phi). \quad (3)$$

The dipole moment of the beam is the current times the displacement and can be written in terms of sine waves as

$$d(t) = ef_0 A \left[\sum_{n+Q>0} \cos(n+Q)\omega_0(t + \tau) + \sum_{n-Q>0} \cos(n-Q)\omega_0(t + \tau) \right]. \quad (4)$$

There are 2 Schottky sidebands per harmonic of the revolution frequency. Each band has a rms amplitude

* Operated by the Universities Research Assoc. under contract no. DE-AC02-76CHO3000 with the US Dept. of Energy

$$P_i = \frac{1}{2} N e^2 A^2 f_0^2. \quad (5)$$

Schottky signals are often observed with a pair of strip-line pickups. The beam current is observed when the top and bottom pickups are added. The dipole moment is obtained when the two pickups are subtracted. An example of the observation of the dipole signal is shown in Fig. 2.

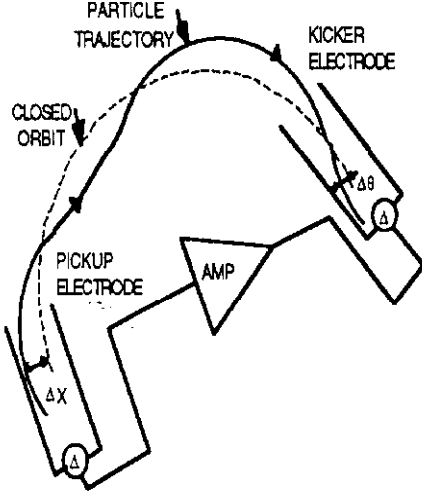


Fig. 1. Schematic of a typical stochastic cooling system. The particle position is sensed at the pickup and a corresponding deflection is applied at the kicker.

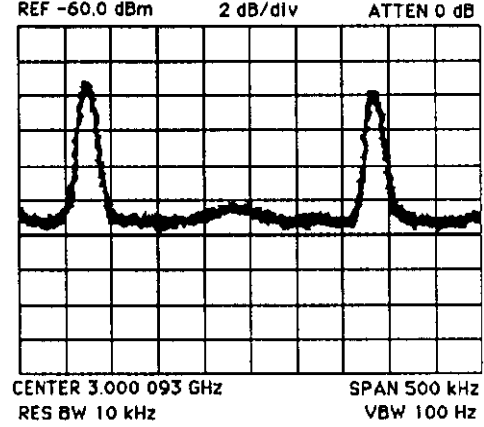


Fig. 2. The Schottky signal from the two betatron sidebands in the FNAL Debuncher ring is shown. The pickup is most sensitive to the dipole moment but has some direct sensitivity to the current which produces a small enhancement at harmonics of the revolution frequency as seen near the center of the trace.

1.2 Action of the Feedback

We consider the action of the feedback system in Fig. 1 on a coasting beam. A more schematic representation is shown in Fig. 3. The dipole moment will be the sum of the dipole moment $d_i(\omega)$ in the absence of the feedback system and a dipole moment $d_f(\omega)$ induced by the excitation applied to the kicker. If this excitation is not too large, then the dipole moment will depend linearly on the deflection.

$$d_f(\omega) = F(\omega)\theta(\omega). \quad (6)$$

We further assume that the angular deflection depends linearly on the dipole moment of the beam:

$$\theta(\omega) = G(\omega)[d_i(\omega) + d_f(\omega)]. \quad (7)$$

Using the circuit shown in Fig. 3, one can infer that

$$\begin{aligned} \theta(\omega) &= \frac{G(\omega)d_i(\omega)}{1 - F(\omega)G(\omega)} \\ &= H(\omega)d_i(\omega). \end{aligned} \quad (8)$$

Fig. 3 and this formalism are intended to demonstrate that stochastic cooling is formally identical to purely electronic feedback circuits. Thus, one can apply the techniques used in dealing with these more commonplace feedback circuits directly to stochastic cooling systems. Network analyzers can be effectively employed to measure the denominator in Eq. (8). The denominator, in fact, is of considerably more importance than the numerator. Not only does it determine system stability according to the criterion of Nyquist [8], it also provides a measure of the cooling rate relative to the maximum rate that can be obtained.

In order to understand the relationship between the denominator of Eq. (8) and the cooling effect, consider Fig. 4. A segment of a beam is shown in coordinate space. Suppose that a random clumping of particles gives the beam a net dipole moment near the center of the beam. The action of the stochastic cooling

system serves to reduce the dipole moment by displacing the centroid of the beam by making the "kink" shown in Fig. 4. This effect of the cooling system is known as "signal suppression." When signal suppression is present, the motion of the beam centroid produces a signal which is opposite in sign to the Schottky signal. If the cooling system is turned off, the Schottky signal will return to its former level.

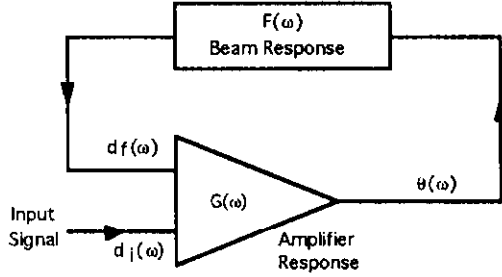


Fig. 3. Equivalent circuit of the beam feedback. The input signal d_j is modified by the addition of the feedback df .

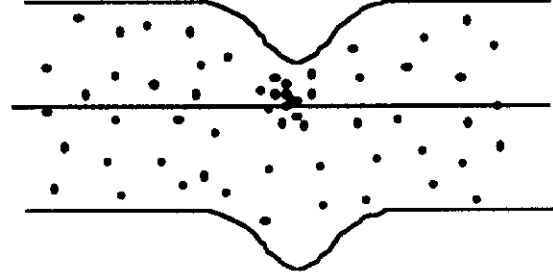


Fig. 4. A cartoon of the behavior of a fluctuation in the dipole moment of the beam under the influence of a stochastic cooling system.

The kink in the beam reduces the amplitudes of the particles that constitute the clump of beam. These particles have slightly different revolution frequencies, so the clump will dissipate as time elapses. After the clump dissipates these particles will continue to have their reduced amplitudes – even if the cooling system is turned off. Note that some particles have their amplitudes increased in this process. However, the net effect is beam cooling since more particles are in the clump of beam than outside it. The length of time that it takes for fluctuations to disappear is defined to be M times the revolution period, where M is known as the mixing factor. Large values of M reduce the maximum cooling rate. The power of the cooling system to resolve two nearby fluctuations is approximately $1/W$, where W is the cooling system bandwidth.

1.3 Betatron Cooling

In order to quantitatively connect the signal suppression phenomenon and the cooling rate, consider the equations of motion. The emittance is a constant of motion in the absence of the cooling system. Under the action of the cooling system the change in amplitude of the i^{th} particle is:

$$\begin{aligned}\Delta(A_i^2) &= \frac{\beta}{2} [(\theta_i + \Delta\theta)^2 - \theta_i^2] \\ &= \beta\theta_i\Delta\theta + \frac{\beta}{2}\Delta\theta^2,\end{aligned}\quad (9)$$

where β is the beta function at the kicker, θ_i is the angle of the i^{th} particle at the kicker, and $\Delta\theta$ is the angular deflection at the kicker. The deflection at the kicker depends linearly on the signals the various particles created at the pickup. Therefore one can write the deflection as a sum over particles

$$\Delta\theta = \sum_{j=1}^N \Delta\theta_j,\quad (10)$$

where $\Delta\theta_j$ is contribution of the motion of the j^{th} particle to the total deflection. We can use Eqs. (9) and (10) to compute the change in emittance as follows:

$$\Delta\varepsilon = \frac{1}{N} \sum_{i=1}^N \Delta(A_i^2) = \frac{\beta}{2N} \sum_{i=1}^N (2\theta_i\Delta\theta_i + N\Delta\theta_i^2).\quad (11)$$

In writing Eq. (11) it has been assumed that the particle motions are random, so that the $i \neq j$ terms do not on the average contribute to $\Delta\varepsilon$ and the double sum collapses to a single sum.

An evaluation of $\Delta\theta$ and a more detailed account of some other significant points are given in reference 7. The result is that the cooling rate is given by

$$\frac{1}{\epsilon} \frac{d\epsilon}{dt} = \frac{1}{4\pi N} \sum_{i=1}^N \omega_{oi} \sum_{n=-\infty}^{\infty} \left\{ -2 \operatorname{Re} \left[jH((n+Q)\omega_{oi}) e^{j\mu_k} e^{-j(n+Q)\omega_{oi}t_k} \right] \right. \\ \left. + \left[M((n+Q)\omega_{oi}) + U((n+Q)\omega_{oi}) \right] \left| H((n+Q)\omega_{oi}) \right|^2 \right\}, \quad (12)$$

where Q is the betatron tune, μ_k is the phase advance between pickup and kicker, ω_{oi} is the angular revolution frequency, and t_k is the transit time delay between pickup and kicker. The first term on the right hand side of Eq. (12) is the cooling term. The cooling rate is maximized when $\mu_k = \pi/2$ and $H(\omega)$ is real except for a phase factor $e^{j(n+Q)\omega_{oi}t_k}$. The phase factor corresponds to a delay equal to the particle pickup to kicker delay.

The mixing factor M is the ratio of the Schottky power density of particles with the same revolution frequency as the i^{th} particle to the average Schottky power. Since no particles have *exactly* the same revolution frequency as the i^{th} particle, the calculation of M must be understood as a limit. If the cooling is applied for a time T , the number of particles that have a revolution frequency that is indistinguishable from the i^{th} particle is proportional to $1/T$. The growth in amplitude squared from the remaining particles, however, is proportional to T^2 . Thus the net effect on the i^{th} particle is a growth in amplitude squared that is linear with time.

The factor $U(\omega)$ is the ratio of thermal noise power to the average Schottky power. It enters into the equations in exactly the same way as the Schottky power. The only difference between the Schottky noise and thermal noise is that the system designer has some control over the value of the thermal noise. In fact, in low density beams the major design challenge may be to achieve an acceptable signal to noise ratio.

Since the cooling term in Eq. (12) is proportional to $H(\omega)$ and the heating term is proportional to $|H(\omega)|^2$, there is a value of H that achieves the highest cooling rate. This value is known as the optimum gain. Gain values which exceed the optimum gain will result in a reduced cooling rate.

Equation (12) is the exact expression for cooling in the frequency domain. The cooling of particles with different frequencies will vary because of the differences in the phase factors in the cooling term and the mixing factor M . The cooling system is usually phased for the center of the beam distribution – where M usually has a peak. The heating term decreases as the frequency departs from the center, but the phase error of the cooling term increases so the cooling rate doesn't vary too much. It is conventional to estimate the cooling rate by using the cooling value at the peak value of M . If H is at the optimum gain, the formula for the cooling rate becomes:

$$\frac{1}{\epsilon} \frac{d\epsilon}{dt} = \frac{W}{N(\overline{M} + \overline{U})}, \quad (13)$$

where $W = f_{\max} - f_{\min}$ is the cooling system bandwidth and \overline{M} and \overline{U} are the peak values of M and U .

1.4 Momentum Cooling

Momentum cooling is similar to betatron cooling except that a technique is required to develop a signal that is proportional to the momentum of the particle. The simplest technique is to place a difference pickup in a region of non-zero dispersion. A pickup that measures the dipole moment of the particles in a region of dispersion will produce a Schottky voltage proportional to the momentum fluctuations in the beam. This voltage can be made to accelerate or decelerate the beam in a kicker and therefore cool the momentum spread. This cooling method is sometimes called the Palmer method. A second technique is to use a notch filter. The filter response changes sign depending on whether the particle revolution frequency is above or below the desired frequency. This method of cooling [9] is sometimes called the Thorndahl method.

The two methods have disadvantages and advantages. The pickup placed in the region of dispersion will have poor signal to noise ratio (nominally 0) at the center of the pickup. The notch filter method avoids the low signal to noise ratio by filtering the noise as well as the signal, and the signal to noise ratio follows the particle density throughout the notch. The filter method can only be used if the revolution frequency versus momentum relationship is unique (non-overlapping Schottky bands). The filter introduces undesirable phase characteristics that reduce the cooling rate. Thus, the filter method is used in situations where the signal to noise ratio is critical; otherwise the pickup in dispersion is used.

Momentum cooling is conventionally described by a Fokker-Planck equation. The beam is described by a distribution $N(E,t)$, which is the number of particles having energy greater than E at time t . The density Ψ is given by

$$\Psi(E,t) = \frac{\partial N(E,t)}{\partial E}, \quad (14)$$

and the flux is given by

$$\Phi(E,t) = \frac{\partial N(E,t)}{\partial t}. \quad (15)$$

The flux is related to the beam distribution by the Fokker-Planck equation

$$\Phi = F\Psi + (D_0 + D_1 + D_2\Psi) \frac{\partial \Psi}{\partial E}. \quad (16)$$

The term proportional to $F = F(E)$ is the cooling term. $F(E)$ is proportional to the cooling system gain G . The term D_1 is a heating term that is proportional to thermal noise in the system. The term proportional to D_2 is the Schottky heating term. The Schottky heating is proportional to $\Psi(E,t)$ the number of particles at that energy (or equivalently that revolution frequency). Both D_1 and D_2 are proportional to G^2 . The term D_0 is used to describe external heating mechanisms such as intrabeam scattering that are independent of cooling system gain.

One can describe momentum cooling in terms of moments similar to the equation describing betatron cooling. However, moments tend to be less useful because of the non-linear nature of Eq. (16): as the cooling proceeds the density increases and the Schottky heating term increases. Similarly, one can write a Fokker-Planck equation to describe betatron cooling. However, most betatron cooling applications are fairly well described by gaussian distributions where the variation in the rms beam size completely describes the beam evolution. Momentum cooling, however, has been applied to antiproton momentum stacking, working with non-gaussian distributions. Eq. (16) can be solved analytically for a number of situations where $\Phi(E,t) = \Phi_0 = \text{constant}$. A solution for antiproton stacking is discussed by van der Meer [10].

1.5 Good and Bad Mixing

Perhaps the most fundamental limitation in achieving effective cooling comes from limitations in the mixing. The fastest cooling is achieved if the Schottky signal is completely randomized between successive passes through the pickup. The randomization is complete in the limit that $M = 1$. However, the Schottky signal should not change between pickup and kicker (M should be large). The randomization between successive passes through the pickup is sometimes called the "good mixing" and the randomization between pickup and kicker is sometimes called the "bad mixing". A reasonable rule of thumb is that $M=3$ for an optimized betatron cooling system.

Antiproton sources CERN AA and FNAL Accumulator were engineered to have a specific value of mixing by using appropriate magnetic lattice design techniques. The lattice parameter $\eta = 1/\gamma_i^2 - 1/\gamma^2$ specifies the spread in revolution periods. At a particular frequency in the cooling band the time spread in revolution frequencies leads to phase errors. As the frequency is increased, the phase error increases. Thus, attempts to upgrade the antiproton source cooling systems are constrained by the limitation imposed by the "bad mixing." At other accelerators it is a matter of luck if the lattice parameter η is appropriate for effective cooling at some frequency.

Possible solutions to the mixing problem are special lattices that have no mixing between pickup and kicker and yet have large mixing between kicker and pickup. Such a lattice was considered at least briefly as a possible design for the CERN Antiproton Collector, but I do not know of any accelerator built on this principle. Another possibility is to design a special pickup placed in a region of dispersion to cancel the transit time differences of the particles in the beam. The basic idea is that both the transit time difference and the position at the pickup are proportional to the momentum offset. If the signal at the pickup can be made to have a time delay that is proportional to the horizontal position of the particle, it may be possible to have the time delay difference in the pickup exactly compensate the pickup to kicker transit time difference.

2. TECHNOLOGY

2.1 Bandwidth considerations

Stochastic cooling systems have been built with bandwidths ranging from 100 MHz to 4 GHz. The highest frequency systems operate in the 4-8 GHz band. Systems typically are chosen to operate in a band where the upper frequency is twice the lower frequency (known as an octave bandwidth). It becomes extremely difficult for a variety of technological reasons to maintain uniform gain amplitude and phase over bands that exceed one octave.

From a technological point of view it appears possible to extend present stochastic cooling technology to frequencies in the 10's of GHz. Aside from the good mixing/bad mixing problem mentioned above some of the technical difficulties in extending the frequency range of stochastic cooling systems are discussed below.

2.2 Pickups and Kickers

Pickups are devices that convert the mechanical beam energy into electrical energy. Kickers perform work on the beam with the applied electrical energy. The same structure can act as either a pickup or a kicker. The reciprocity theorem states that any device that converts the mechanical energy of the beam into electrical energy can be used to convert electrical energy into mechanical energy with the same coupling. A more precise statement of this theorem and other theoretical and practical pickup considerations can be found in the article by Lambertson [11]. The major practical differences between pickup and kicker design is that pickups may be cooled to cryogenic temperatures to reduce the thermal noise level while kickers may be required to dissipate significant rf power.

2.3 Stripline Pickup Response Model

Although other types of pickups are possible [12,13], the most common pickup is the strip-line type indicated in Figs. 5 and 6. These figures are also intended to suggest an electrical model of the beam current and stripline. The beam current is given by:

$$i(z, t) = i_0 e^{j(kz - \omega t)} \quad (17)$$

where $v = \omega / k$ is the beam velocity. A current equal in magnitude but opposite in sign (the image current) flows on the walls of the beam chamber. A fraction f of the image current flows onto the strip line at one end and off at the other end. The pickup response can be modeled as a transmission line with the beam acting as a current source at the two ends. The solution of these equations shows that the output voltage is given by

$$V_p = f Z_p i_0 \sin kl \quad (18)$$

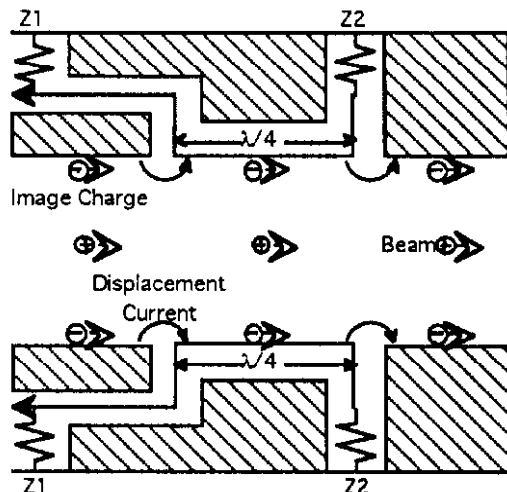


Fig. 5. Schematic representation of a quarter-wave stripline electrode interacting with a high energy charged particle (side view).

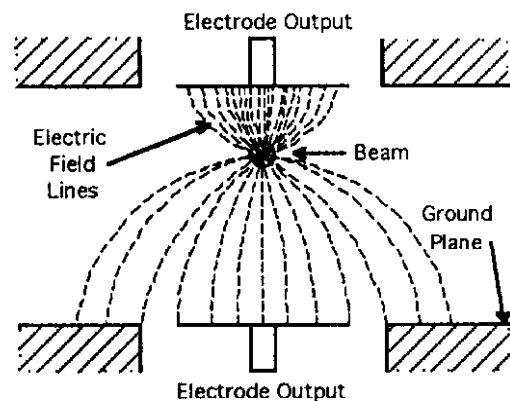


Fig. 6. The electric field lines from a single particle in the vicinity of a pickup electrode. More field lines terminate on the upper plate because the particle is closer to it than to the lower plate (cross-section).

The peak in the response occurs at $kl = \pi/2$. Thus the length is chosen to be a 1/4 wavelength long at the band center frequency. The fraction f of image current that is sensed by the pickup may be estimated by assuming that the pickup is infinitely long in z and solving the following wave equation for the scalar potential:

$$\left(\frac{1}{c}\right)^2 \frac{\partial^2 \Phi}{\partial t^2} - \nabla^2 \Phi = \rho(x, y) e^{j(kz - \omega t)} \quad (19)$$

where $\rho(x, y)$ is the beam density. Writing the potential as:

$$\Phi = \Theta(x, y) e^{j(kz - \omega t)} \quad (20)$$

the equation for the potential becomes

$$\nabla_t^2 \Theta - \left[k^2 - \left(\frac{\omega}{c}\right)^2 \right] \Theta = \rho(x, y) \quad (21)$$

For some simple geometries Eq. (21) can be solved analytically. If b is the transverse dimension of the beam chamber and $kb \ll 1$, the term in the [] is small and can be neglected. Under these conditions Eq. (21) reduces to the 2-dimensional Poisson's equation, and it can be solved by any of a large arsenal of techniques. The image currents are obtained by integrating the normal component of the electric field over the surface of the pickup.

2.4 Design Considerations

Schottky signal beam currents are often small compared to the noise current from thermal fluctuations. Arrays of 100 or more pickups are commonly used to obtain an adequate signal to noise ratio. The output power of two pickups is conveniently combined by connecting them to transmission lines of the same characteristic impedance as the pickup. The two transmission lines can be joined together and they will transmit all their power to a transmission line of half the impedance (assuming that the transmission lines are of the proper length so that the signals arrive in phase where the lines are joined). The transmission line with half the characteristic impedance can be transformed to a higher impedance with a series of stepped 1/4 wavelength transmission lines (or a single tapered line) and the combination process can be cascaded several times. This technique is easily implemented for bandwidths of an octave or less using stripline or microstrip circuit board techniques. In fact, the need for extensive combiner boards has recently led to the construction of the pickups themselves by using standard printed circuit board techniques [14,15]. These techniques have substantially reduced the cost of building pickup and kicker arrays.

Since the signal level tends to be low, it is important to maximize the signal seen by each individual pickup. Since the beam is an excellent current source, the signal is maximized by using a high impedance pickup. Typical pickup impedances are in the range 50-100 Ω . In principle, one can obtain larger impedances by leaving the electrode dimensions fixed and increasing the wall dimensions indefinitely. However, the impedance only increases logarithmically for large wall dimensions. Furthermore, unless the frequency is very low, the electrode would not act much like a transmission line since its height would greatly exceed its length.

The electrode sensitivity is also maximized by using wide electrodes to intercept a large fraction of the image currents (see Fig. 6). If the beam chamber is small or the energy is high, the electric field will be transverse and the currents at a given z will all be in phase. However, the energy from different parts of the electrode may be collected with slightly different transit times. The resulting phase errors are likely to be a limiting factor in the performance of large electrodes in the GHz region.

2.5 Wave Guide Modes

Another problem in the design of pickups is suggested by Eq. (21). The general solution of this equation is any solution of the inhomogeneous equation plus the general solution of the homogeneous equation. The solution of the homogeneous equation is the well-known infinite set of wave guide modes. The solution becomes mathematically unique if one applies boundary conditions at the two ends of cylinder. Physically, these wave guide modes arise from discontinuities in the beam chamber. The discontinuities are excited by the beam current and then radiate energy into the wave guide modes.

The presence of wave guide modes causes two problems. The wave guide modes propagate with velocities that depend on frequency and are different from the beam velocity. Thus, it tends to be difficult to use them for cooling over a significant bandwidth because of the large and unpredictable phase errors that are present with these modes. Even more annoying is the fact that these modes may show resonant behavior – especially if the pickup chamber is not well matched in cross-section to the rest of the beam chamber. In this case, there may be a peak in the amplitude of the gain function $G(\omega)$ and a corresponding rapid change in phase of 180° or more. This situation inevitably leads to system instability at gains lower than the optimum cooling gain.

There are two defenses against undesired microwave modes. The first comes naturally when many pickups are combined. The pickups are phased for the beam velocity. The microwave modes are rejected because their propagation velocities are different (typically slower). The second defense is to place microwave absorbers in the pickup. Possible absorbers include bulk and film resistors, lossy dielectrics, and lossy magnetic materials.

2.6 Limitations to Pickup Sensitivity at High Frequencies

The most fundamental limitation on building pickups that are sensitive to Schottky signals at very high frequency is the reduction in wall current intensity at high frequency. To illustrate the point, consider Eq. (21) for a beam in a circular pipe of radius b . The charge density $\rho(x, y)$ is assumed to be uniform for radii less than a . It is straight-forward to show that the radial electric field at the beam chamber wall is:

$$E_r(b) = \frac{\rho_0 a I_1(k'a)}{\epsilon_0 k' b I_0(k'b)} e^{j(kz - \omega t)} \quad (22)$$

where ρ_0 is the uniform charge density, I_0 and I_1 are modified Bessel's functions, $k' = k / \gamma$, $\gamma = \sqrt{1 - (v/c)^2}$, and $\epsilon_0 = 8.85 \times 10^{-12}$ F/m. Equation (22) reduces to a $1/\text{radius}$ dependence for $k' \rightarrow 0$. However, the electric field falls exponentially with asymptotically large k' . This asymptotic condition is avoided by either $b \rightarrow 0$ or $\gamma \rightarrow \infty$. Thus the cutoff frequency is an important limitation for high frequencies, large apertures, and low energies. For example, $I_0(k'b) = 1.2$ at $k = 0.6 \text{ cm}^{-1}$, $b = 5 \text{ cm}$, and $\gamma = 3.7$, which are approximately the parameters that correspond to the stochastic cooling systems at the CERN Antiproton Collector Ring.

2.7 Amplifier and Resistor Noise Minimization

In many cooling systems the signal to noise ratio is a significant concern. Maximizing the number and sensitivity of the pickups is crucial to obtain an adequate signal. Other techniques are available to reduce the thermal noise. The thermal noise comes from two sources which are comparable in magnitude: the back termination in the pickup and the preamplifier itself. The thermal noise voltage $V_n = 2\sqrt{k_B T R}$ from the resistance R at temperature T is easy to characterize. Normally R is chosen to be the characteristic impedance of the system (50Ω). If one makes R smaller, then the system is mismatched and the noise power will be a function of frequency. The noise power in the frequency band of interest may be reduced by this technique. A more universally applicable technique is to lower the resistor temperature. Resistors are cooled to cryogenic temperatures extensively at both the CERN and FNAL antiproton sources. The physics of low noise amplifiers is considerably more complicated – and certainly beyond my understanding. Fortunately, there is a large industry working on making low noise microwave amplifiers, so the problem of being clever is reduced to the more tractable problem of being adequately funded.

2.8 Filters and Equalizers

Filters are used extensively in stochastic cooling systems. One type of filter is intended to have a shape that repeats (more or less) each Schottky band. These filters are used, for example, to suppress noise or shift the phase of the cooling signal. A simple filter that is used extensively at the FNAL antiproton source is shown in Fig. 7. The output transfer function is the sum of a prompt and a delayed signal: $T(\omega) = (1 - e^{j\omega\tau}) / 2$, where τ is the difference in length between the short and long legs.. This type of filter has transmission zeroes when $\omega\tau = 2\pi$ and is sometimes referred to as a "notch filter." Other types of notch filters are possible: the stack tail filters at the AA utilize shunt transmission lines. However, all these filters require one or more elements that delay the signal by a multiple of τ , where $1/\tau = 4f_0$, and f_0 is the average revolution frequency. In order for the filter to work properly the delay elements must be accurately described by a pure delay, i.e., the attenuation and the group delay must be independent of frequency. Thus, the problem of building a periodic filter is essentially that of building an ideal transmission line.

A number of transmission line techniques can be used. The simplest technique uses coaxial cable as the delay element. The diameter of the cable must be large to avoid large attenuation. The skin and dielectric losses are inversely proportional to the radius. The skin loss increases with the square root of the frequency. The dielectric loss is more complicated but tends to increase with frequency also. However, the size of the coaxial cable is limited because of the need to avoid the lowest wave guide mode (TM_{01}). While it is possible to calculate the cutoff frequency for the mode, the effect of non-propagating modes can be significant depending on the construction of the cable. Thus, the maximum usable frequency of a cable is best determined by measurements. The combination of increasing skin losses and being forced to smaller diameter cable can be very dramatic. For example, foam dielectric 7/8 inch heliax cable can be used up to a frequency of 5 GHz where it has a power transmission of 7% over a distance of 100 m, but a similar 3/8 inch cable has a power transmission of 0.001% at 11 GHz [16].

Fortunately other techniques are available. One technique used at the FNAL antiproton source involves the use of super-conducting delay lines to avoid the skin losses [17]. Another technique involves amplitude modulation of a laser coupled to an optical fiber followed by demodulation using a photo diode at the far end of the fiber [18,19]. Very long (10's of μsec) delays are possible with this technique. Bulk acoustic wave (BAW) devices have been more recently used to replace the super-conducting delay lines at FNAL to achieve lower operational costs [20]. Both the BAW and the optical modulation techniques suffer from large inefficiencies in converting energy from one form to another.

Equalizers are filters that have nearly constant gain over a single Schottky band. They are used, for example, to attenuate low frequencies to compensate for the high frequency attenuation that occurs in cables and other devices. Equalizers are extensively used commercially, and they may be conveniently constructed of strip-line or microstrip. A number of computer aided design programs can be used to accurately predict performance and to take most of the guess work out of equalizer design. Typically a stochastic cooling system will be built and the gain measured with an open-loop gain measurement (see below). Then an equalization filter will be constructed to flatten the gain and phase [21].

3. TECHNIQUES

3.1. Open-loop gain measurements

One of the most important diagnostic measurements made on a stochastic cooling system is a measurement of the open-loop gain. A typical experimental setup for this type of measurement is shown in Fig. 8. The cooling system is opened at some point and a sine-wave excitation is applied to the portion of the system leading to the kicker. The signal is transmitted via the beam, detected by the pickup, and brought back to the point of excitation. The propagation delay along the signal path ($T_1+T_4+T_3$) is equal to the difference in cooling system delay and beam transit time ($T_2-T_1-T_3$) plus one revolution period. Since the revolution period contributes a 360° phase shift, the open-loop gain measurement measures directly and precisely the transit time difference between the electronic signal and the beam motion.

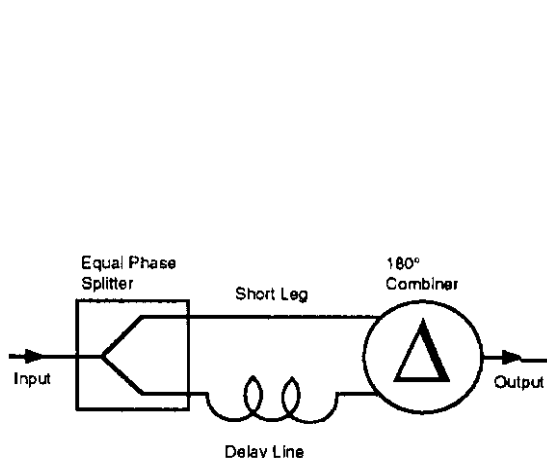


Fig. 7. Schematic of a simple filter of the type used in the FNAL antiproton source.

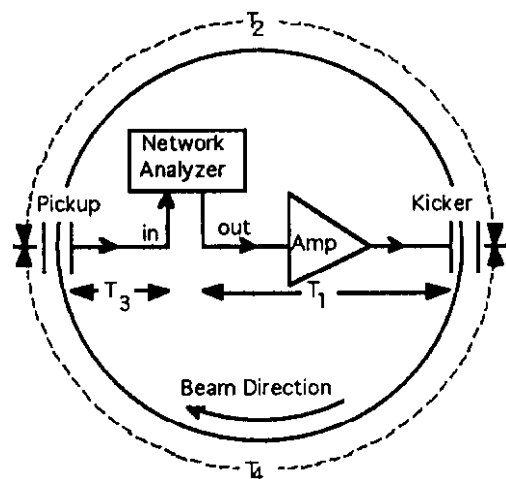


Fig. 8. Schematic of a typical setup for a cooling system open-loop gain measurement.

The open-loop gain measures the quantity $F(\omega)G(\omega)$ in Eq. (8). An open-loop gain measurement is shown in Fig. 9. The structure of the curves is dominated by the beam response since $G(\omega)$ is nearly constant

over the narrow frequency range in this measurement. There are four peaks in the amplitude corresponding to the four betatron sidebands inside the frequency interval that was measured. Each peak is accompanied by a rapid 180° change in phase. The phase at the peaks of the amplitude response is 180° when $G(\omega)$ is phased for cooling. The data in Fig. 9 indicate a phase at the peaks of the betatron sidebands of around 90° , so the phase of this system is not properly adjusted to achieve cooling.

In order to get more information about $G(\omega)$, it is useful to measure many Schottky bands. Normally, this measurement is accomplished by measuring a few points per Schottky band and measuring 100 or so Schottky bands throughout the frequency range of the cooling system. Such a measurement is shown in Fig. 10. The phases and amplitudes of the upper and lower sidebands are shown separately. It can be seen that the phases of these bands are slightly different. This difference occurs because the phase advance between pickup and kicker is not exactly an odd multiple of 90° . The amplitude curves give a good estimate of the phase and relative amplitude of $G(\omega)$. Data like those in Fig. 10 are useful in designing equalizers that can be used to optimize the cooling rate.

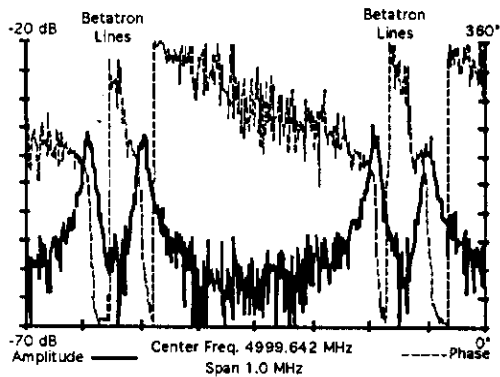


Fig. 9. Open-loop gain of a 4 to 8 GHz betatron cooling system at the FNAL Accumulator ring. The revolution frequency is 629 kHz. The four peaks correspond to the four betatron peaks that lie in the 1-MHz interval. The phase changes rapidly by 180° in the vicinity of the amplitude peaks.

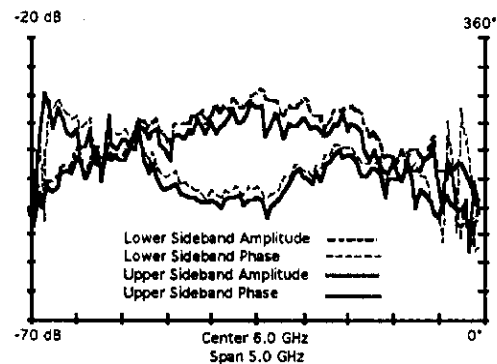


Fig. 10 Open-loop measurement of the same system shown in Fig. 9. One point is measured on every 40^{th} betatron line. The average phase is about 180° , as required for cooling.

3.2 Schottky signal suppression

Since the cooling system works using the Schottky signal it is useful, if not essential, that one be able to monitor the Schottky signal at some point in the stochastic cooling system. With these observations one can measure the signal to noise ratio and the mixing factor.

The phenomenon of Schottky signal suppression (discussed above) is an especially useful diagnostic. A signal suppression amplitude of 6 dB indicates that the system is operating at the optimum gain. The measurement is made by observing the difference between the open-loop and closed-loop Schottky signal. A measurement showing about 6 dB of signal suppression is shown in Fig. 11. The closed-loop response in Fig. 11 is lower than the open-loop noise floor. This phenomenon occurs because the beam response acts to cancel a portion of the electronic noise. Signal suppression measurements are particularly useful to check the operation of cooling systems where the cooling rate is very slow and difficult to measure directly.

3.3. Cooling rate

There are a large number of ways of directly measuring the cooling rate. One commonly used method is to observe the rate of change of the Schottky signal. In addition to providing the cooling signal, Schottky signals can be used to measure the momentum spread, tune, transverse beam size, and chromaticity of the beam[22]. An example of the measurement of the horizontal betatron amplitude cooling rate is shown in Fig. 13. The horizontal beam emittance is changed by approximately two orders of magnitude while the beam current and vertical beam emittance are nearly constant. One can avoid the signal suppression effect by observing a Schottky band that is outside the bandwidth of the cooling system.

It is also possible to measure the transverse size of the beam using a variety of other techniques including using flying wires or extracting the beam and measuring the beam shape with segmented ion or secondary emission chambers. Measurements of the profile of the circulating beam were made in the FNAL Debuncher ring by imaging the residual gas that is ionized by the beam. The profiles thus obtained are shown in Fig. 12.

One can determine the optimum system delay for the FNAL Debuncher transverse cooling systems to a few psec by minimizing the width of the beam profile on a secondary emission chamber.

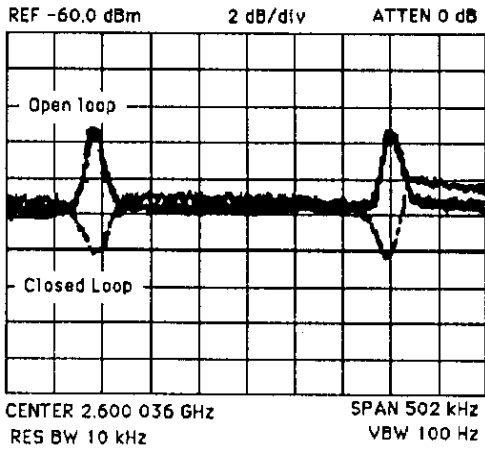


Fig. 11. Spectrum analyzer traces showing the difference between the open-loop and closed-loop signals coming from the pickup.

Fig. 12. Beam profiles in the FNAL Debuncher ring. The profiles were obtained at 0.22-sec intervals. The earliest time is at the top of the plot; the latest, at the bottom.

3.4. Instabilities

The presence of the denominator in the cooling equations suggests the possibility that $1 - F(\omega)G(\omega)$ might vanish, and the system could become unstable. A stability diagram of a betatron cooling system operating near the optimum gain with a pickup to kicker phase advance of 70° is shown in Fig. 14. The system is unstable if the stability curve encircles the value of $+1$ (on the real axis). The two loops on the plot correspond to the two Schottky sidebands. At the frequencies that correspond to the peaks of the betatron sidebands the function is approximately -1 . Between the sidebands the gain is less than 0.2 . Raising the gain of the system a factor of 10 beyond the optimum gain will cause an instability. Of course, any one Schottky band can cause an instability. Variations in gain and phase from one Schottky band to another can erode the margin between the optimum gain and the unstable gain.

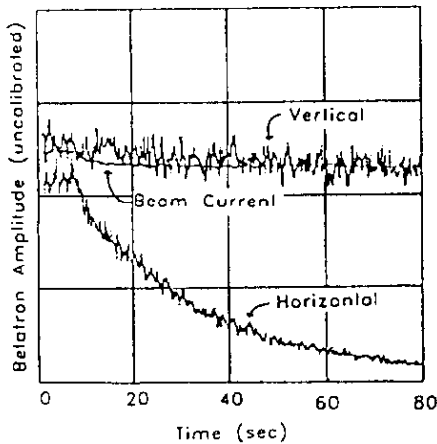


Fig. 13. A spectrum analyzer is tuned to receive the power from a single Schottky band.

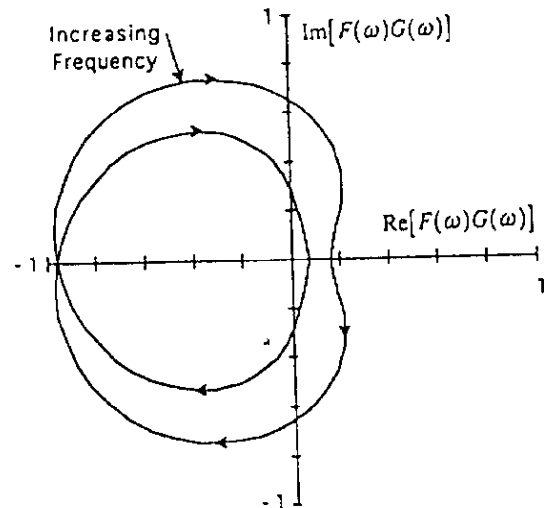


Fig. 14. A stability plot of a betatron cooling system. The plot is drawn for a betatron cooling system at the FNAL accumulator for the frequency range $(n-0.5)f_0$ to $(n+0.5)f_0$, with $n=5000$ and $f_0=629$ kHz.

CONCLUSION

The theory, technology, and techniques of stochastic cooling have been reviewed. Where possible I have tried to indicate the limitations of our current techniques and technology.

REFERENCES

- [1] D. Mohl, G. Petrucci, L. Thorndahl, and S. van der Meer, Phys. Rep. **58**, 73 (1980).
- [2] J. Bisognano and C. Leeman, **AIP Conf. Proc. 87**, Physics of Particle Accelerators, Fermilab Summer School 1981, Ed. R.A. Carrigan, et al., American Institute of Physics, New York, 1982, p 583.
- [3] S. Chattopadhyay, IEEE Trans. Nucl. Sci. **30**, 2649 (1983).
- [4] J.J. Bisognano, **AIP Conf. Proc. 127**, Physics of Particle Accelerators, BNL/SUNY Summer School 1983, Ed. M. Month et al., American Institute of Physics, New York, 1985, p 443.
- [5] N.S. Dikanskii and D.V. Pestrikov, Sov. Phys. Tech. Phys. **29**, 271 (1984).
- [6] D. Mohl, Proceedings, Advanced Accelerator Physics, Oxford, 1985, Vol 2, p.453.
- [7] Marriner JP, McGinnis D, **AIP Conf. Proc. 249**, Physics of Particle Accelerators, Eds. M Month and M Dienes, American Institute of Physics, New York, 1992, p 693.
- [8] H. Nyquist, Bell S. Tech. J., **11**, 126 (1932).
- [9] G. Carron G and L. Thorndahl, CERN Internal Report, CERN-ISR-RF/78-12 (1978)
- [10] S. van der Meer, CERN Internal Report, CERN/PS/AA/78-22 (1978).
- [11] Lambertson, G., **AIP Conf. Proc. 153**, Physics of Particle Accelerators, SLAC Summer School 1985, Fermilab Summer School 1984, Vol. II, Ed. M. Month and M. Dienes, American Institute of Physics, New York, 1987, p. 1414.
- [12] L. Faltin, Nucl. Instr. Meth., **A241**, 416 (1985).
- [13] G. Di Massa, Nuovo Cim., **100A**, 249 (1988).
- [14] F. Caspers, IEEE Trans. on Nucl. Sci., **34**, 1866 (1987).
- [15] J. Petter et al., Proceedings of the IEEE Particle Accelerator Conf. (Chicago), Vol. 1, 636 (1989).
- [16] Andrew Corporation, Catalog 35, Orland Park, IL, USA.
- [17] R.J. Pasquinelli, Proceedings of the 12th International Conference on High-Energy Accelerators (Fermilab), p 584 (1983).
- [18] J.D. Simpson and R. Konecny, IEEE Trans. Nucl. Sci. xxx, 2129 (1985).
- [19] R. Pasquinelli, Proceedings of the 1989 IEEE Particle accelerator Convergence (Chicago), Vol 1, p 694.
- [20] R. Pasquinelli, Conf. Rec. of the 1991 IEEE Particle Accelerator Conf. (San Francisco), Vol. 3, p. 1395 (1991).
- [21] D. McGinnis, Conf. Rec. of the 1991 IEEE Particle Accelerator Conf. (San Francisco) Vol 3, p. 1392.
- [22] S. van der Meer S, CERN Internal Report, CERN/PS/88-60 (AR), (1988).